Dual modulation of unitary L-type Ca^{2+} channel currents by $[Ca^{2+}]_i$ in fura-2-loaded guinea-pig ventricular myocytes

Yuji Hirano and Masayasu Hiraoka

Department of Cardiovascular Diseases, Medical Research Institute, Tokyo Medical and Dental University, 1-5-45, Yushima, Bunkyo-ku, Tokyo 113, Japan

1. Single-channel studies were performed to clarify how tonic changes in intracellular Ca^{2+} concentrations ($[Ca^{2+}]_i$) modulate cardiac L-type Ca^{2+} channels. Currents were recorded from fura-2-loaded guinea-pig ventricular myocytes in the cell-attached configuration. Fura-2 fluorescence signals were recorded simultaneously during pulses to elicit channel activity.

2. The myocyte $[Ca^{2+}]_i$ was altered through changes in bath Ca^{2+} concentration during K^+ depolarization. When $[Ca^{2+}]_i$ exceeded ~2 times the resting level (estimated $[Ca^{2+}]_i$ around 180–400 nM), the activity of Ca^{2+} channels was reversibly potentiated without changes in unitary current amplitudes.

3. Increased channel open probability during Ca^{2+}-dependent potentiation resulted from increased availability and increased open probability during non-blank sweeps. Closed time analysis revealed a distribution best fitted with two exponentials. Increased $[Ca^{2+}]_i$ reduced the longer time constant, but had no effect on the shorter time constant. The open time constant was unchanged in most cases. Current records occasionally included sweeps with long openings (~10 ms or more), whose appearance increased during potentiation.

4. When $[Ca^{2+}]_i$ was increased after cAMP-dependent upregulation of Ca^{2+} channels, the change in channel activity was diminished. Similar results were observed when Ca^{2+}-dependent potentiation was examined in myocytes exposed to a membrane-permeant protein kinase inhibitor, H-89. This suggests that channel phosphorylation may be responsible for Ca^{2+}-dependent potentiation.

5. When $[Ca^{2+}]_i$ was further increased, but remained below the threshold for contraction (estimated $[Ca^{2+}]_i$ above 600 nM), Ca^{2+} channel activity was suppressed.

6. Our results demonstrate directly at the single-channel level that $[Ca^{2+}]_i$ modulates the activity of cardiac L-type Ca^{2+} channels, enhancing it with modest $[Ca^{2+}]_i$ increases and decreasing it with greater $[Ca^{2+}]_i$ increases.

Voltage-dependent L-type Ca^{2+} channel activity in neurons and muscle is regulated by neurotransmitters, hormones and various intracellular factors (Reuter, 1983; Tsien, Bean, Hess, Lansman, Nilius & Nowycky, 1986; Trautwein & Hescheler, 1990). A rise in intracellular calcium concentration ($[Ca^{2+}]_i$) is known to inactivate Ca^{2+} channels in many cell types, resulting in control of Ca^{2+} influx through a negative feedback mechanism (Eckert & Chad, 1984; Kass & Sanguinetti, 1984; Lee, Marban & Tsien, 1985; Romanin, Karlsson & Schindler; 1992). Increase in $[Ca^{2+}]_i$, however, can show an opposite effect when the rise in $[Ca^{2+}]_i$ is limited. A positive feedback mechanism or $[Ca^{2+}]_i$-induced potentiation of Ca^{2+} current has been suggested or supported by different lines of investigations in cardiac myocytes (Marban & Tsien, 1982; Fedida, Noble & Spindler, 1988; Tseng, 1989; Zygmunt & Maylie, 1990) and has been demonstrated at the whole-cell current level using caged-Ca^{2+} compounds (Gurney, Charnet, Pye & Nargeot, 1989; Hadley & Lederer, 1991; Bates & Gurney, 1993). In spite of these observations, the mechanisms of $[Ca^{2+}]_i$-induced modulations and the interrelationships between the two opposite effects of $[Ca^{2+}]_i$ on Ca^{2+} current are not yet fully clarified. It is also unclear at what levels of $[Ca^{2+}]_i$ these two functions take place. Furthermore, in contrast to the case of inactivation (Imredy & Yue, 1992; Romanin *et al.* 1992) $[Ca^{2+}]_i$-induced potentiation has not yet been characterized at the single-channel current level. In the present study, we recorded unitary L-type Ca^{2+} channel currents from guinea-pig ventricular myocytes in cell-attached configuration, while simultaneously recording fura-2 fluorescence to monitor the changes in $[Ca^{2+}]_i$. Our results provide direct evidence

at the single-channel level that $[Ca^{2+}]_i$ modulates the activity of Ca^{2+} channels in two opposite ways, depending on its concentration.

METHODS

Preparations

Ventricular myocytes from guinea-pig hearts were obtained by an enzymatic dissociation procedure similar to that described previously (Isenberg & Klockner, 1982; Hirano & Hiraoka, 1988). Briefly, guinea-pigs weighing 250–350 g were anaesthetized with sodium pentobarbitone (30 mg kg^{-1}, I.P.). The chest was opened and the aorta was cannulated *in situ* to be perfused with Tyrode solution, before the heart was removed. Hearts were then retrogradely perfused with low-Ca^{2+} (30 μM) Tyrode solution with collagenase (0·4 mg ml^{-1}, type I, Sigma) for 20 min using a Langendorff apparatus. After the enzyme was washed out, the cells were dissociated in high-K^+, low-Cl^- storage solution.

$[Ca^{2+}]_i$ measurement

Cells were loaded with fura-2 (Grynkievicz, Poenie & Tsien, 1985) by exposure to 5 μM acetoxymethylester form (fura-2 AM) in high-K^+, low-Cl^- solution for 40 min at 20 °C (Hirano, Abe, Sawanobori & Hiraoka, 1991). Cells were washed and then stored in dye-free medium for at least 1 h. This step gave time for cells to convert the indicator from the AM form to the free acid form. Cells were then placed in a small experimental chamber mounted on the stage of an inverted microscope equipped with epifluorescence optics (Diaphoto TMD, Nikon, Tokyo). $[Ca^{2+}]_i$ was monitored using a dual-wavelength fluorometer (CAM-230, Japan Spectroscopic, Tokyo). Fluorescence was excited at wavelengths of 340 nm (F_{340}) and 380 nm (F_{380}) alternately using the rotating sector mirror method, with the chopper frequency set at 400 Hz. The emission of fluorescence (wavelength 500 nm) was measured from a single rectangular area of the cell image. Signals from the photomultiplier tube were sampled and processed by a CAM-230 chopper system to yield two fluorescence intensities (F_{340} and F_{380}) separately. They were filtered by resistance–capacitance (RC) circuits with a time constant set to 10 ms.

To minimize cell damage due to the fluorescence excitation, illumination was limited to the period when the A/D converter was in sampling mode for the current and optical signals. During the course of long experiments, there was occasionally a gradual decrease in F_{340} and F_{380} (up to 10% in 1 h). Autofluorescence of myocytes (as estimated from unstained cells) was still negligible in these conditions (less than 5% of total fluorescence).

There are a number of problems in the determination of absolute values of $[Ca^{2+}]_i$ from fura-2 signals, especially when fura-2 is loaded in the AM form (Wier 1990; Frampton, Orchard & Boyett, 1991). We have tried to estimate $[Ca^{2+}]_i$ levels based on an *in vivo* calibration technique (Li, Altschuld & Stokes, 1990; Frampton *et al.* 1991). Briefly, cells loaded with fluorescent probes were superfused with a glucose-free solution containing carbonyl cyanide *m*-chlorophenylhydrazon (CCCP, 5 μM, Sigma) and rotenone (5 μM, Sigma) for 20 min to deplete stores of intracellular ATP. After the maximum ratio (R_{max}) was determined by adding the Ca^{2+} ionomycin (20 μM, Sigma) and $CaCl_2$ (5 mM), the minimum ratio (R_{min}) was obtained by changing the solution to that containing ionomycin (20 μM) and EGTA (10 mM). The value of β, i.e. the fluorescence intensity ratio of Ca^{2+}-free and Ca^{2+}-saturated conditions measured at a wavelength of 380 nm, could also be estimated during this procedure (see legend to Fig. 1). $[Ca^{2+}]_i$ is then related to the fluorescence ratio (R) according to the following equation:

$$[Ca^{2+}]_i = K_d \beta (R - R_{min}) / (R_{max} - R),$$

where K_d is the dissociation constant for the Ca^{2+}–fura-2 complex. We assumed a value of 200 nm for K_d (Williams, Fogarty, Tsien & Fay, 1985). Thus, we obtained the calibration curve of our system, shown in Fig. 1*A*. The absolute $[Ca^{2+}]_i$ value, however, should be taken with caution because of the need to assure a value of K_d and other problems described in detail by Frampton *et al.* (1991). It should be noted that the estimate of K_d is linearly related to the estimate of $[Ca^{2+}]_i$.

With several possible uncertainties in the calibration procedure in mind, we have chosen to use the fluorescence ratio ($R_{340/380}$) to indicate the changes in $[Ca^{2+}]_i$ in the Results section. Also, we have supplemented the calibration procedure by the measurement of the fluorescence ratio of myocytes during K^+ depolarization in Tyrode solution containing 1·8 mM Ca^{2+} (Fig. 1*B*). Comparison with these data might be helpful to evaluate the physiological significance of the changes in $R_{340/380}$ observed in this study, because this is free from the assumption on the value of K_d.

Electrophysiological measurement and data analysis

Single-channel currents were recorded in the cell-attached configuration (Hamill, Marty, Neher, Sakmann & Sigworth, 1981) using an Axopatch-1D amplifier (Axon Instruments, Foster City, CA, USA). Pipettes were pulled from capillary tubes in the two-step process, coated with insulating varnish, and fire-polished afterwards. When filled with the Ba^{2+} solution, the pipette had a resistance of 4–8 MΩ. The membrane potential of myocytes was near 0 mV with exposure to a high-K^+ solution. Because of the surface charge effect produced by a high concentration of divalent cations in the pipette, the activation voltage for Ca^{2+} channels in this study is shifted in the positive direction compared with that under physiological conditions (see Hirano, Fozzard & January, 1989, for example). Without correction for a liquid junctional potential between the pipette and bath solution (−12 mV in our case; see Ochi & Kawashima, 1990), the threshold for the activation of L-type Ca^{2+} channel currents was around −10 mV. Because changes in channel activity at fixed membrane potentials are the focus of this study, membrane potentials in this study are presented without correction for the junctional potential, as is customary in similar published studies. From the holding potential of −80 mV, patches were depolarized at 0·5 or 1 Hz to 0, +10 or +20 mV for 180 ms. Current signals were filtered at 1 kHz (−3 dB; 8-pole Bessel filter). They were digitized at 5 kHz along with fura-2 fluorescence data, and stored in a computer (PC9801RA, NEC, Tokyo). After digital subtraction for capacitive and leak components, idealized records obtained by standard half-height criteria were used to calculate the channel open probability (P_o or NP_o). Fittings for open or closed time distributions were mostly done using pCLAMP software (Axon Instruments) on an IBM PS2 personal computer, after data file conversion into pCLAMP compatible format. Where appropriate, data are reported as means ± S.D. Differences in the numerical values between two groups were evaluated using Student's *t* test.

Solutions

The Ca^{2+}-free bath solution contained (mM): potassium aspartate, 120; KCl, 20; glucose, 10; EGTA, 2; and Hepes, 10 (adjusted to pH 7·4 with KOH). Ca^{2+}-containing bath

solutions were prepared by adding $CaCl_2$ (2 mM in Figs 2–7 and 2·5 mM in Figs 8 and 9) to the calcium-free bath solution. The pipette solution contained (mM): $BaCl_2$, 100; and Hepes, 10 (adjusted to pH 7·4 with TEA-OH). The normal Tyrode solution contained (mM): NaCl, 143; KCl, 4; $MgCl_2$, 0·5; glucose, 5·5; $CaCl_2$, 1·8; NaH_2PO_4, 0·33; and Hepes, 5 (adjusted to pH 7·4 with NaOH). High-K^+ Tyrode solutions in Fig. 1*B* were obtained by replacing NaCl with equimolar KCl. Fura-2 AM was from Dojin Inc. (Kumamoto, Japan). The protein kinase inhibitor, H-89 (*N*-[2-((3–4-bromophenyl)-amino)-ethyl]-5-isoquinonlinesulphonamide), was from Seikagaku Kogyo Co. (Tokyo). All other chemicals were obtained from Sigma.

RESULTS

Ca^{2+}-dependent potentiation

Simultaneous recordings of Ca^{2+} channel current and fura-2 fluorescence signals in this study were carried out from myocytes exposed to 140 mM K^+ solutions (see above). After seal formation, stability of channel activity was confirmed by recording unitary current for 10 min in the absence of intervention. When control high-K^+, Ca^{2+}-free bath solution was switched to high-K^+, Ca^{2+}-containing solution, a gradual increase in the F_{340} and decrease in the F_{380} signals were observed, indicating an increase in $[Ca^{2+}]_i$. With bath solution containing 2 mM EGTA and 2 mM Ca^{2+} (calculated $[Ca^{2+}]_o \approx 10\ \mu M$), $R_{340/380}$ typically reached 0·5–0·8 and reversed when bath solution was returned to the control Ca^{2+}-free solution. This was used as the standard procedure to observe Ca^{2+}-dependent potentiation in this study.

Figure 2 shows a case when change in $[Ca^{2+}]_i$ was reversed. Original traces, consisting of current and optical signals, are shown in Fig. 2*A*. From these data, two fluorescence intensities (F_{340} and F_{380}), their ratio ($R_{340/380}$) and channel open probability (NP_o) were obtained for every sweep given at 1 Hz. As shown in the upper panel in Fig. 2*B*, the application of Ca^{2+}-containing bath solution for about 10 min caused a rise in $R_{340/380}$ to nearly 0·8 from the control value of 0·3. Upon return to the Ca^{2+}-free solution, the ratio returned to the control value. To show

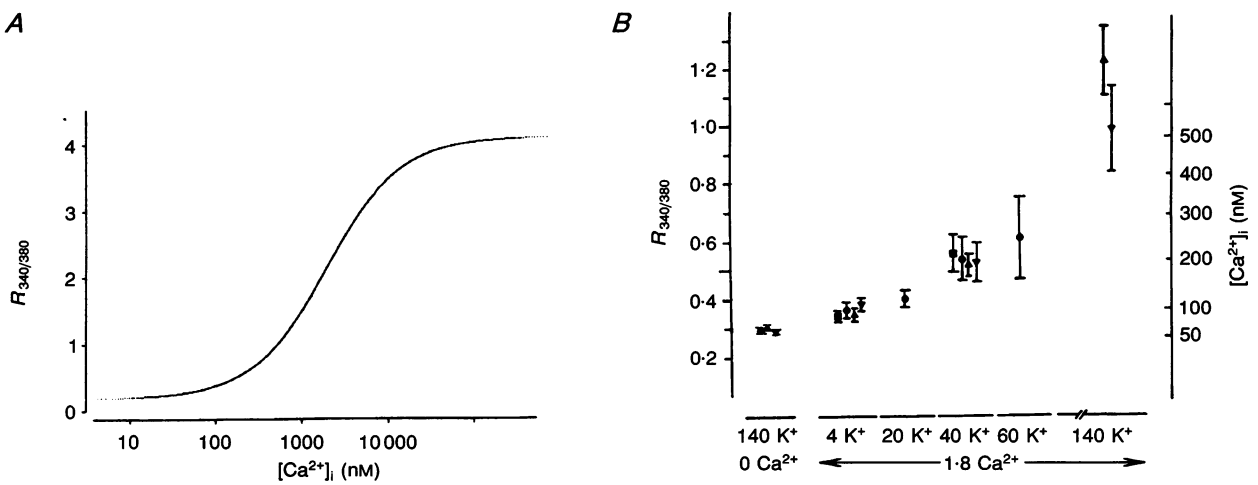

Figure 1. Estimation of absolute values of $[Ca^{2+}]_i$

A, calibration curve for fura-2 signals, as determined from the data in permeabilized guinea-pig ventricular myocytes. The curve was drawn according to the following equation (Grynkievicz *et al.* 1985): $[Ca^{2+}]_i = K_d\beta(R - R_{min})/(R - R_{max})$, where $K_d = 200$, $\beta = 10$, $R_{max} = 4{\cdot}1$ and $R_{min} = 0{\cdot}19$. Constants required for calibration were obtained from ATP-depleted cells as described in the text. Results from 3 myocytes were: 4·3, 3·9 and 4·1 for R_{max}; 0·185, 0·22 and 0·19 for R_{min}; and 11·2, 8·4 and 10·3 for β. These values for R_{max} and R_{min} *in vivo* were lower than those obtained from thin layer of Mops (3-(*N*-morpholino)propanesulphonic acid)-buffered 100 mM K^+ solutions (pH 7·0) containing fura-2 (10 μM) and 2 mM-Ca^{2+} (R_{max}, 5·9) or fura-2 and 10 mM-EGTA (R_{min}, 0·23). *B*, fluorescence ratio during K^+ depolarization. $R_{340/380}$ was measured from myocytes exposed to the solutions indicated at the bottom (concentrations are mM). Averaged values of $R_{340/380}$ are plotted with their S.D. values. Different symbols indicate that data were obtained on different occasions. Corresponding $[Ca^{2+}]_i$ values on the right are calculated from the calibration curve in *A*. $R_{340/380}$ obtained in control high-K^+, Ca^{2+}-free bath solution ($0{\cdot}29 \pm 0{\cdot}01$, $n = 19$) was slightly lower than that in resting $[Ca^{2+}]_i$ level in normal Tyrode solution with 1·8 mM $CaCl_2$ ($0{\cdot}35 \pm 0{\cdot}03$, $n = 40$). When K^+ was raised to 40 mM, $R_{340/380}$ reached $0{\cdot}53 \pm 0{\cdot}07$ ($n = 41$) and was stable during the 10 min observation period. When myocytes were exposed to 140 mM K^+ solution with 1·8 mM Ca^{2+}, they initially showed spontaneous contractions with $R_{340/380}$ values around 1·5–2·0. Most of the myocytes then became quiescent without detectable cell contracture. $R_{340/380}$ values in this figure were obtained from these quiescent cells.

values averaged for every five sweeps are plotted in the lower panel. Numbers in the bottom give NP_0 values averaged over every 250 sweeps. They increased when $R_{340/380}$ was raised. The increased NP_0 then declined as $R_{340/380}$ was decreased, indicating the reversibility of $[Ca^{2+}]_i$-induced potentiation of Ca^{2+} channel activity. This response, however, seemed to be associated with delay compared to changes in $[Ca^{2+}]_i$, based on the following observations. (1) Averaged NP_0 values were largest in the seventh segments when $R_{340/380}$ returned to below 0·4. (2) NP_0 for the last segment was still larger than control values. Similar findings with persistent effects or short-term 'memory' in Ca^{2+}-dependent potentiation were observed in three additional patches.

When $R_{340/380}$ was raised above 0·5, $[Ca^{2+}]_i$-induced potentiation was a consistent finding in all the patches examined. We summarized our data in Fig. 3 by plotting how changes in $R_{340/380}$ produced an increase in channel activity in the same patches, where current records of more than 250 sweeps were obtained at a stable level of fluorescence ratio. After the number of channels in the patches were taken into consideration, control P_o values at each test potential still showed considerable variation. As described below, we found diverse patterns of changes in the kinetic behaviour of individual channels during Ca^{2+}-dependent potentiation. Variability in basal channel activity may be responsible for these observations.

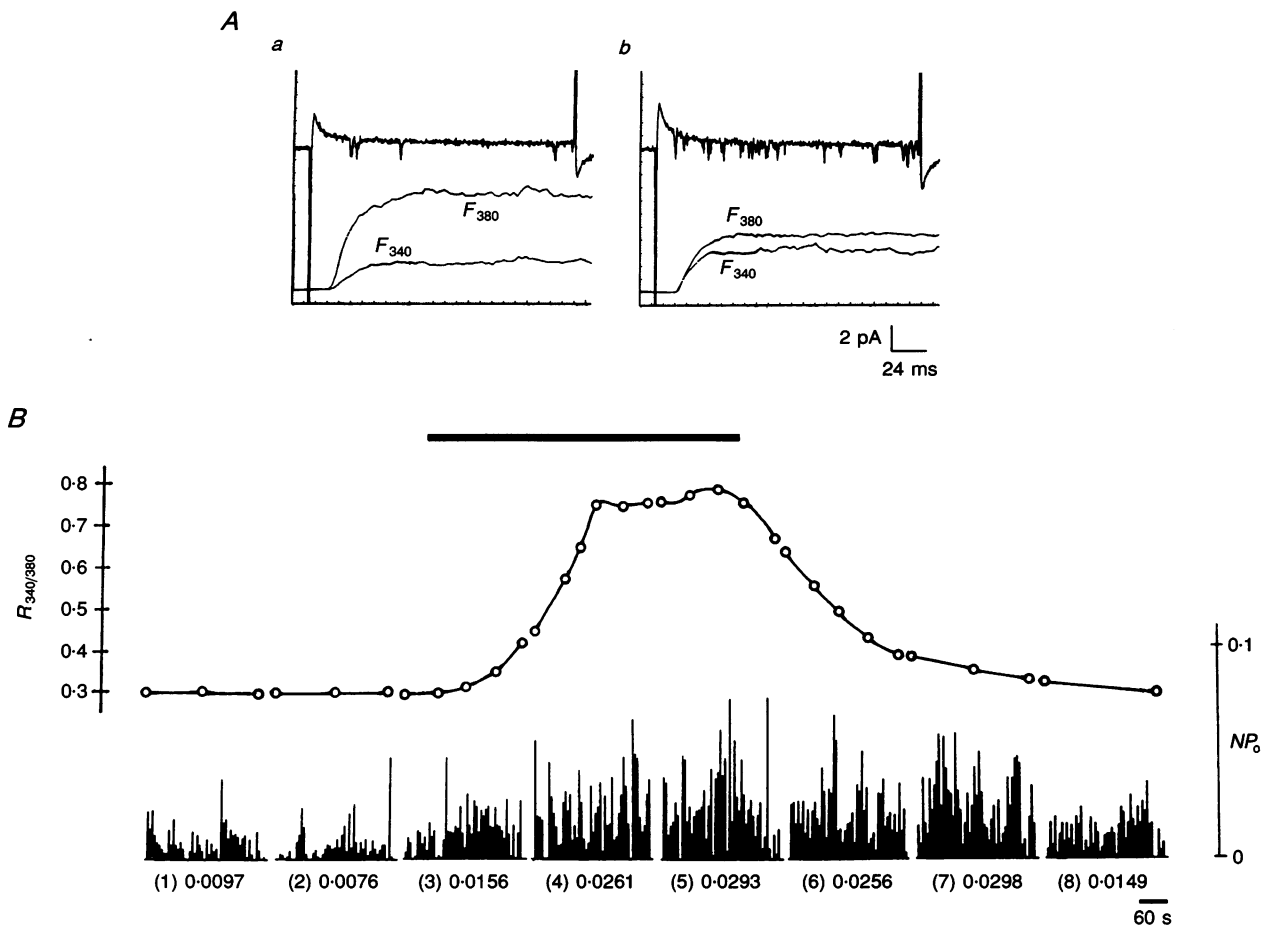

Figure 2. Changes in $[Ca^{2+}]_i$ and channel open probability (NP_0) after bath solution was switched to Ca^{2+}-containing solution

Data consist of 8 segments, each containing 250 pulses to 0 mV delivered at 1 Hz. The two panels in *A* show the structure of original data, consisting of current and two optical signals (F_{340} and F_{380}). Delayed responses in optical signals were due to the delay at the mechanical shutter and due to filtration of signals by RC circuits. Averaged values of F_{340} and F_{380} during 90–180 ms from the onset of each sweep were used to obtain fluorescence ratio data ($R_{340/380}$). Panel *a* is taken from the first data segment, while panel *b* is from the fifth segment. *B*, the upper panel shows the temporal profile of $R_{340/380}$. In the lower panel, each bar indicates NP_0 values averaged over every 5 sweeps including 0 for null sweeps. Numbers in the bottom give averaged NP_0 values through each segment (250 sweeps). Period for application of Ca^{2+}-containing bath solution is indicated by the bar at the top.

We examined whether or not the unitary current amplitude of Ca^{2+} channels was affected during Ca^{2+}-dependent potentiation. Figure 4*A* shows a recording at the test potential of +20 mV. We selected sweeps with long openings to construct the amplitude histograms in the control (Fig. 4*A a*) and during Ca^{2+}-dependent potentiation (Fig. 4*A b*). Unitary current amplitudes, as defined by the distance between two peaks in the histogram, were little affected. Figure 4*B* shows results from a different patch, where double-pulse protocols were applied to promote high voltage-induced long openings (Pietrobon & Hess, 1990). Although sweeps with a changed gating mode were observed only on rare occasions, this attempt helped to confirm the stability of unitary current amplitude during Ca^{2+}-dependent potentiation, even at voltage levels where its assessment is difficult due to short channel open times. As shown on the right, channel conductances calculated by current amplitudes at 0 and +20 mV were not affected during Ca^{2+}-dependent potentiation.

Kinetic analysis of single-channel current during Ca^{2+}-dependent potentiation

In several single-channel patches, we could record stable channel activity long enough to allow detailed kinetic analysis. Figure 5 shows temporal profiles of P_o from such cases. Figure 5*A* and *B* are from two different patches depolarized to different test voltages (*A*, + 10 mV; *B*, + 20 mV). When $[Ca^{2+}]_i$ was increased, there was an increase in the number of sweeps with channel activity (non-blank sweeps) in both cases (from 27 to 50% in *A* and from 70 to 84% in *B*). Also, averaged P_o for non-blank sweeps were increased (from 0·04 to 0·10 in *A* and 0·13 to 0·27 in *B*). As shown in Table 1, these two different factors were a consistent finding in our experiments on Ca^{2+}-dependent potentiation.

Non-blank and blank sweeps in Fig. 5 appeared in clusters (Cavalier, Pelzer & Trautwein, 1986). We analysed the changes in these patterns or 'slow gating' as defined by Ochi & Kawashima (1990). In two cases shown here, the average number of consecutive non-blank sweeps (T_s) increased after Ca^{2+}-dependent potentiation (from 2·6 to 3·8 in *A* and from 4·3 to 11·7 in *B*). On the other hand, the average number of consecutive blank sweeps (T_f) decreased from 6·8 to 3·7 in *A*, while changes in *B* were slight and in the opposite direction (from 1·8 to 2·2). In eight cases summarized in Table 1, T_s was significantly increased by 102 ± 70% ($P < 0·05$; mean T_s from 4·04 ± 1·66 to 8·34 ± 5·23) during Ca^{2+}-dependent potentiation. On the other hand, the slight decrease in the duration of T_f by 12·3 ± 38·5% (mean T_f from 3·31 ± 1·72 to 2·49 ± 0·66) was not statistically significant.

We then analysed the distribution of open and closed times, because changes in these properties should be responsible for the increase in average P_o for non-blank sweeps. Figures 6 and 7 are from a single-channel patch where recordings at three different test potentials were successful in the control (*A*), during Ca^{2+}-dependent potentiation (*B*) and after $[Ca^{2+}]_i$ returned to the control level (*C*). Open-time histograms in Fig. 6 could be fitted by single exponentials, when the fitting range was limited to 10 ms. In this patch, we observed only slight increases in open time constants (τ_{open}) during Ca^{2+}-dependent potentiation. As summarized in Table 1, $[Ca^{2+}]_i$-induced changes in τ_{open} showed considerable variations between patches (from minimal changes to an increase by more than 100%). Variation in control τ_{open} values at given potentials should also be noted. When data at different test potentials were combined taking their ratio (τ_{open} during potentiation : τ_{open} in the control) as the index, the averaged ratio value amounted to 1·38 ± 0·55 ($n = 8$). This was not a significant increase at the 0·05 level. Thus, while

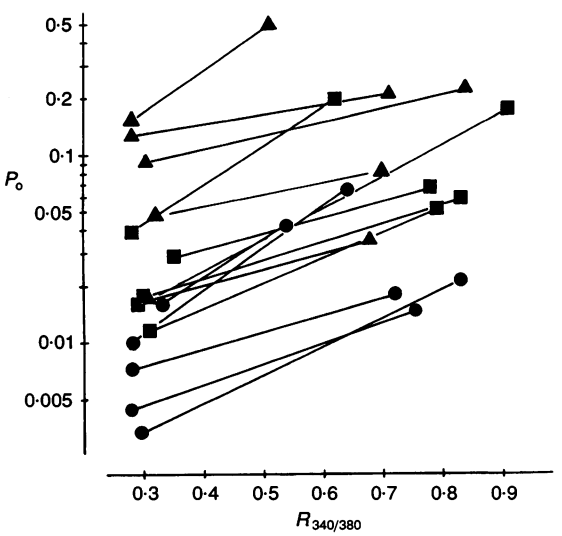

Figure 3. Relationships between $[Ca^{2+}]_i$ and channel open probability
Ordinate, P_o plotted on a logarithmic scale. P_o values were corrected for the number of channels in the patch, as determined by the maximum number of simultaneous openings at depolarization to +20 mV. Abscissa, $R_{340/380}$. Data from the same patch were connected. Different symbols indicate different test voltages (●, 0 mV; ■, + 10 mV; ▲, + 20 mV).

data contained two cases with an apparent increase in τ_{open}, changes in τ_{open} should not be regarded as the main factor contributing to increased P_o during Ca^{2+}-dependent potentiation. Closed time histograms (from the same records as in Fig. 6) are shown in Fig. 7, where the effects of increased $[Ca^{2+}]_i$ were more prominently demonstrated. As in previous reports on the kinetic analysis of Ca^{2+} channels (Fenwick, Marty & Neher, 1982; Cavalier *et al.* 1986), closed time histograms could be fitted by the sum of two exponentials. As shown in Fig. 7, the time constant of the fast exponential was only slightly decreased during Ca^{2+}-dependent potentiation (averaged ratio value = 0·90 ± 0·10 (n = 7), and thus the difference was not significant). On the other hand, that of the slow component ($\tau_{closed,slow}$) was reduced by more than 50% (averaged ratio value 0·47 ± 0·17, n = 7). This factor was the most striking and consistent effect among changes in gating time constants during Ca^{2+}-dependent potentiation. We could confirm the important role for changes in $\tau_{closed,slow}$ in the case shown in Figs 6 and 7. Here, P_o for non-blank sweeps was still at slightly elevated

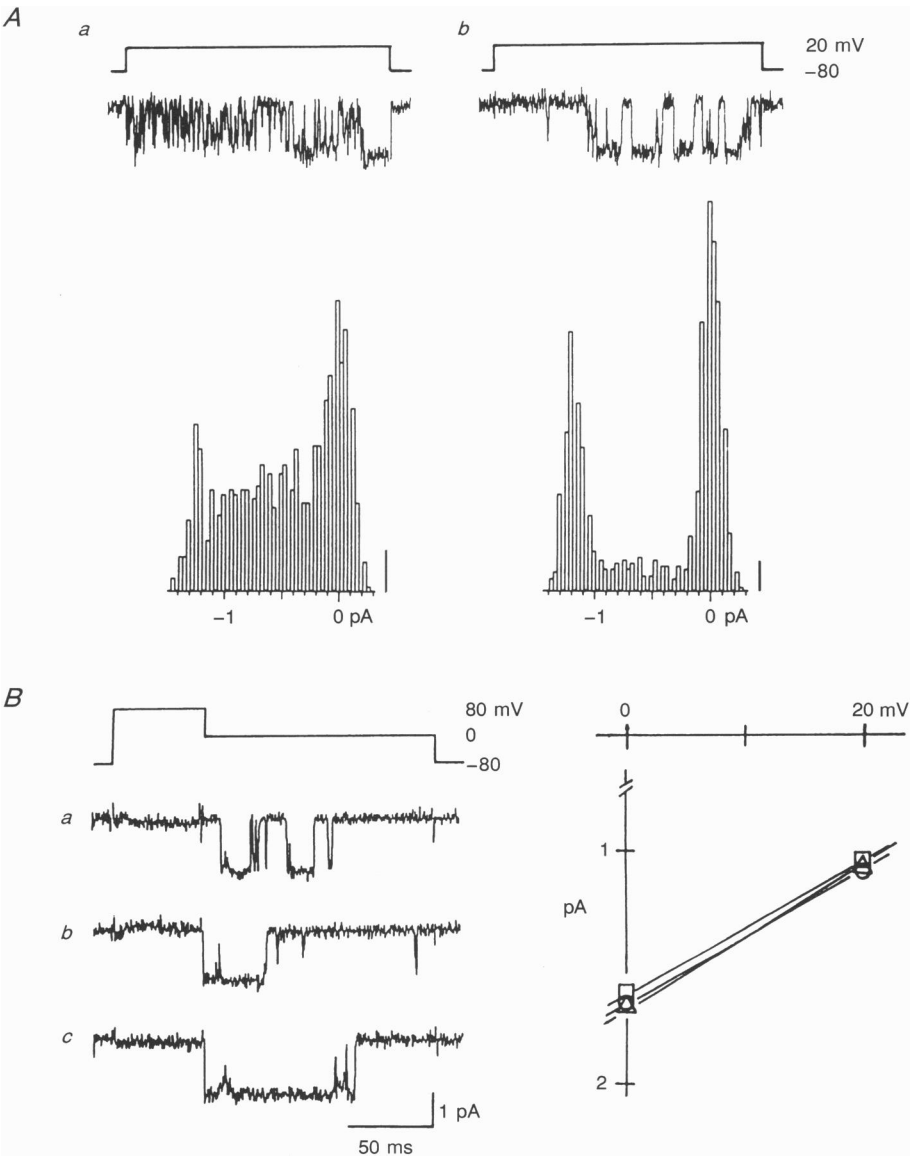

Figure 4. Stationarity of unitary current amplitude during Ca^{2+}-dependent potentiation
A, amplitude histograms in the control (*a*) and during Ca^{2+}-dependent potentiation (*b*). Vertical bars on the right are for 10 counts. In this patch, NP_o increased by 60% as $R_{340/380}$ increased from 0·28 to 0·71. *B*, sweeps with long openings at 0 mV were obtained in the control (*a*), during Ca^{2+}-dependent potentiation (*b*) and after the return to basal $[Ca^{2+}]_i$ levels (*c*). In the right panel, lines connecting unitary current amplitudes at 0 and +20 mV yielded the slope conductance of 27·5 (○, *a*), 27·5 (□, *b*) and 28 pS (△, *c*). Results from the same patch as shown in Figs 6 and 7, where P_o was more than doubled as $R_{340/380}$ increased from 0·30 to 0·83.

levels when $[Ca^{2+}]_i$ returned to the control value (0·13 for *A*, 20 mV, *vs.* 0·19 for *C*, 20 mV, consistent with 'persistent' effects in Fig. 1). This result could be explained by dramatically shortened closed times (Fig. 7*A*, 20 mV *vs.* Fig. 7*C*, 20 mV), because τ_{open} was below the control value when $[Ca^{2+}]_i$ was reduced (Fig. 6*A*, 20 mV *vs.* Fig. 6*C*, 20 mV).

In addition to the contribution by graded changes in gating time constants as described above, we found another factor which contributed to an increase in P_o for non-blank sweeps in several patches recorded at +20 mV. Records during Ca^{2+}-dependent potentiation in Fig. 5*B* included numbers of sweeps with P_o of 0·5 or more. These sweeps often included long openings of Ca^{2+} channels (an example can be seen in the inset of Fig. 6*B*, 20 mV). The number of these long openings was negligible, but their contribution to total current could be substantial. A possible explanation for this observation includes the appearance of 'mode 2' gating as described previously (Hess, Lansman & Tsien, 1984; Yue, Herzig & Marban, 1990; Pietrobon & Hess, 1990; Ono & Fozzard, 1993). In the case analysed in Fig. 6, numbers of sweeps with long openings (duration exceeding 9 ms, i.e. 10 times the τ_{open} in Fig. 6) were six, sixteen and six for recordings at 20 mV in Fig. 6*A*, *B* and *C*, respectively. Figure 8 shows the case where potentiation of long openings was most prominent in our experiments. According to the method proposed by Yue *et al.* (1990), each sweep was characterized by its P_o during depolarization and by the longest open time observed in the corresponding sweep (T_{max}). Thus, the small circles in the $P_o - T_{max}$ plane (Fig. 8) correspond to individual sweeps. During Ca^{2+}-dependent potentiation (*B*), the distribution of sweeps shifted towards increased P_o and prolonged T_{max}, making a more scattered form of distribution. When discriminators were set at $T_{max} = 10$ ms and $P_o = 0{\cdot}1$, the number of sweeps with 'mode 2' gating increased from five to fifty-six. Histogram projections onto the P_o axis (shown below) indicate that Ca^{2+}-dependent potentiation in this case was accompanied by a positive shift of the peak P_o value, located near the centre of the sweep

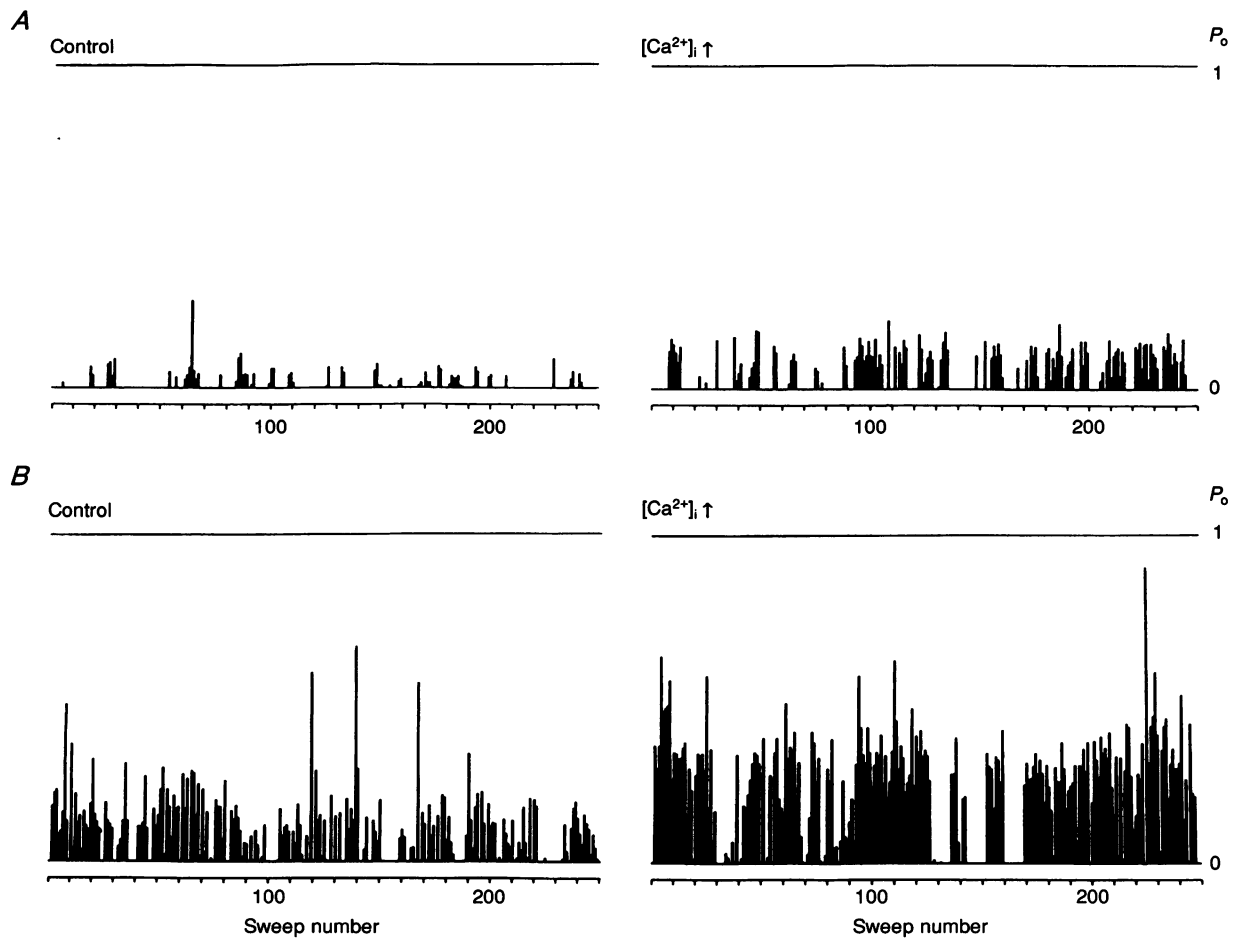

Figure 5. Changes in P_o and channel 'availability' during Ca^{2+}-dependent potentiation
A and *B* were recorded from two different single-channel patches. In each section, P_o values for consecutive 250 sweeps were plotted. An increase in the number of, and the average P_o values for, non-blank sweeps was observed in both cases. In *A*, $R_{340/380}$ was increased from 0·31 to 0·79. *B* is from the same patch as in Figs 6 and 7.

distribution. This type of distribution of P_o with 'mode 2' gating was different from that observed during the application of the dihydropyridine Ca^{2+} agonist, where sweeps are separated into two different clusters (see Fig. 3 in Hess *et al.* 1984).

Combined effects of increase in $[Ca^{2+}]_i$ and protein kinase A stimulation and inhibition

Changes in the kinetic behaviour of Ca^{2+} channels during Ca^{2+}-dependent potentiation described above revealed certain similarities to those during β-adrenergic stimulation (see Discussion). Also, it has been suggested that Ca^{2+}-dependent potentiation in frog atrial cells occurs through cAMP-dependent phosphorylation of the channels (Gurney *et al.* 1989). We therefore examined the interaction between protein kinase A (PKA)-dependent modulation of Ca^{2+} channels and the $[Ca^{2+}]_i$ effects.

Figure 9*A* shows the changes in channel activity when an increase in $[Ca^{2+}]_i$ was introduced after the bath-application of isoprenaline (2 μM), 8-bromocyclic-AMP (2 mM) or forskolin (5 μM) to elevate intracellular cAMP levels. Following cAMP-dependent potentiation, an increase in $[Ca^{2+}]_i$ failed to evoke the potentiation of channel activity in two out of five cases. This finding is in a sharp contrast to the cases without intervention (Fig. 3), where an increase in P_o was a consistent finding. Thus, our results indicate that Ca^{2+}-dependent and cAMP-dependent potentiation are not fully 'additive'. The diminished $[Ca^{2+}]_i$ effects in Fig. 9*A* support the view that Ca^{2+}-dependent potentiation and cAMP-dependent potentiation might involve common mechanisms, at least partly.

We then examined the effects of phosphorylation inhibition. In this series of experiments, data were obtained from myocytes treated by the membrane-permeant protein kinase inhibitor H-89 (1 μM) for 60 min (see Ono & Fozzard, 1993, for the case of rabbit ventricular myocytes). Under these conditions, averaged P_o at +20 mV ($0{\cdot}037 \pm 0{\cdot}012$, $n = 3$) was less than half of the value without intervention ($0{\cdot}088 \pm 0{\cdot}056$, $n = 8$). In preliminary experiments, exposure to H-89 for 20 min was not enough to evoke definite effects on channel activity and a subsequent increase in $[Ca^{2+}]_i$ caused Ca^{2+}-dependent potentiation in two out of two patches. Figure 9*B* shows the results obtained under the condition of protein kinase inhibition by H-89 (incubation for 60 min). We can see that Ca^{2+}-dependent potentiation was largely suppressed in the continued presence of H89.

Table 1. Summary of kinetic analysis during Ca^{2+}-dependent potentiation

Test voltage	$R_{340/380}$	Total P_o	Availability (%)	T_s	T_f	P_o*	τ_{open}	$\tau_{closed,fast}$	$\tau_{closed,slow}$
0 mV	0·30	0·003	34·8	2·63	4·94	0·009	0·39	—	—
	0·83	0·021	74·8	6·68	2·33	0·028	0·44	—	—
10 mV	0·30	0·018	65·6	3·73	2·00	0·027	0·47	0·71	16·0
	0·83	0·057	80·4	9·57	2·23	0·057	0·49	0·68	4·52
	0·31	0·012	26·8	2·58	6·78	0·043	0·27	0·89	6·73
	0·79	0·050	50·4	3·82	3·65	0·099	0·31	0·63	3·42
	0·35	0·028	55·2	3·63	3·03	0·051	0·43	0·58	8·03
	0·78	0·065	71·6	4·84	1·91	0·090	0·52	0·57	5·08
	0·29	0·016	43·6	2·53	3·28	0·036	0·38	0·55	9·70
	0·91	0·168	66·4	4·15	2·10	0·252	0·93	0·51	2·48
20 mV	0·30	0·092	70·4	4·29	1·80	0·131	0·90	0·45	4·98
	0·83	0·226	84·0	11·7	2·22	0·269	0·92	0·46	1·73
	0·32	0·048	70·4	5·87	2·47	0·068	0·46	0·42	5·07
	0·70	0·080	76·0	6·33	2·07	0·105	0·45	0·36	3·20
	0·28	0·156	71·4	7·07	2·19	0·205	0·49	0·63	3·14
	0·51	0·482	87·2	19·6	3·40	0·559	1·02	0·55	2·04

In each section, data from the same patches are tabulated, upper for control and lower during Ca^{2+}-dependent potentiation. Availability is the ratio of the number of non-blank sweeps to total number of sweeps (250 for all the cases here). P_o* is averaged P_o for non-blank sweeps. T_s is the average number of consecutive non-blank sweeps. T_f is the average number of consecutive blank sweeps. Depolarizing pulses were given at 1 Hz in all cases. As described in the text, open time histograms were fitted by single exponentials and closed time histograms by the sum of two exponentials. τ values are given in milliseconds. Numbers of events in the data obtained at 0 mV were not enough for reliable double exponential fittings.

Ca^{2+}-dependent inactivation

We observed that Ca^{2+} channel activity was suppressed when $R_{340/380}$ exceeded the value around unity, which were obtained by raising extracellular Ca^{2+} concentrations. In the case shown in Fig. 10, Ca^{2+}-free bath solution was switched to that containing 2 mM EGTA and 2·5 mM-Ca^{2+} (calculated $[Ca^{2+}]_o \approx 500\ \mu M$). This caused possible potentiation of channel activities during the period when increase in $R_{340/380}$ was up to 0·7. A further increase then reversed the effect to suppression. When the $R_{340/380}$ value passed unity, channel openings became rare, although they were not completely suppressed. Figure 11 shows another case with increased $[Ca^{2+}]_o$ (2 mM EGTA and 2·5 mM Ca^{2+}), where $R_{340/380}$ showed spontaneous fluctuations. As shown in Fig. 11*B*, Ca^{2+}-dependent potentiation was apparent during the period when increase in $R_{340/380}$ was moderate (around 0·8). When $R_{340/380}$ crossed the level of 1·0 several times, the correlation between $R_{340/380}$ and NP_o was inverted compared with those described in previous sections. Here, channel activities were suppressed as $R_{340/380}$ increased, forming a mirror-like image with almost identical time courses. This is in contrast with the cases during Ca^{2+}-dependent potentiation, where the increase in NP_o lagged behind the change in $[Ca^{2+}]_i$ (see Fig. 2). When channels recovered from Ca^{2+}-dependent suppression as $R_{340/380}$ fell below unity again (indicated by *d* in Fig. 11*B*), their activities were not at the control levels (Fig. 11*A*). Instead, they were closer to the level stimulated by a previous 'moderate' increase in $[Ca^{2+}]_i$ (*b* in Fig. 11*B*). This observation suggests that Ca^{2+}-induced potentiation

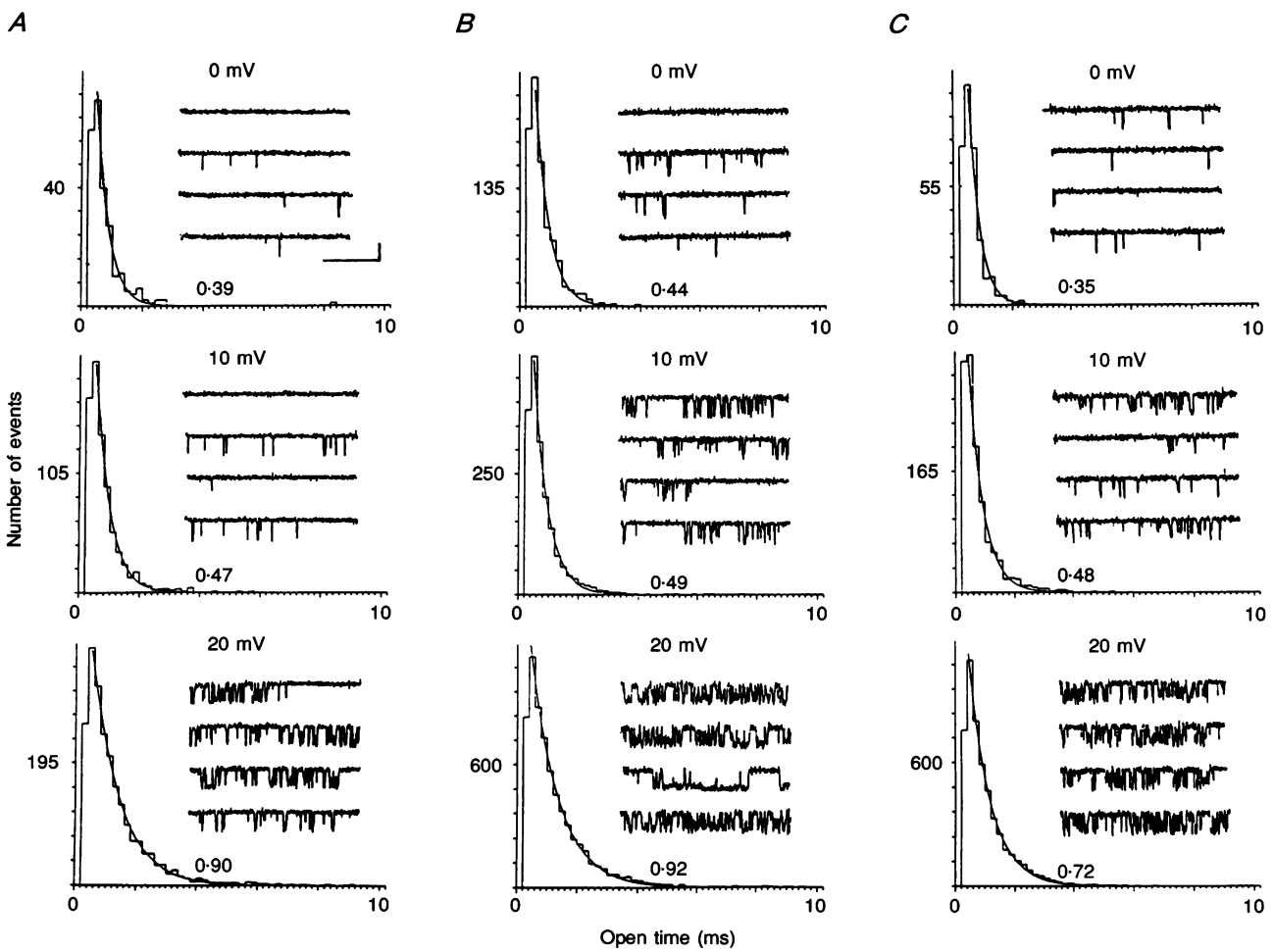

Figure 6. Open time histograms
Records were obtained by depolarization to 0, +10 and +20 mV before (*A*), during (*B*) and after (*C*) superfusion by Ca^{2+}-containing bath solution. Although *C* was recorded during the period when $R_{340/380}$ returned to the control levels, total open probability was still in slightly potentiated levels (0·005, 0·025 and 0·133 for 0, 10 and 20 mV, respectively). Numbers in each panel indicate τ_{open} in milliseconds, obtained by single exponential fittings. Four consecutive sweeps from corresponding files are shown in the inset of each panel, with calibration bars in the top panel of *A* for 1 pA and 60 ms.

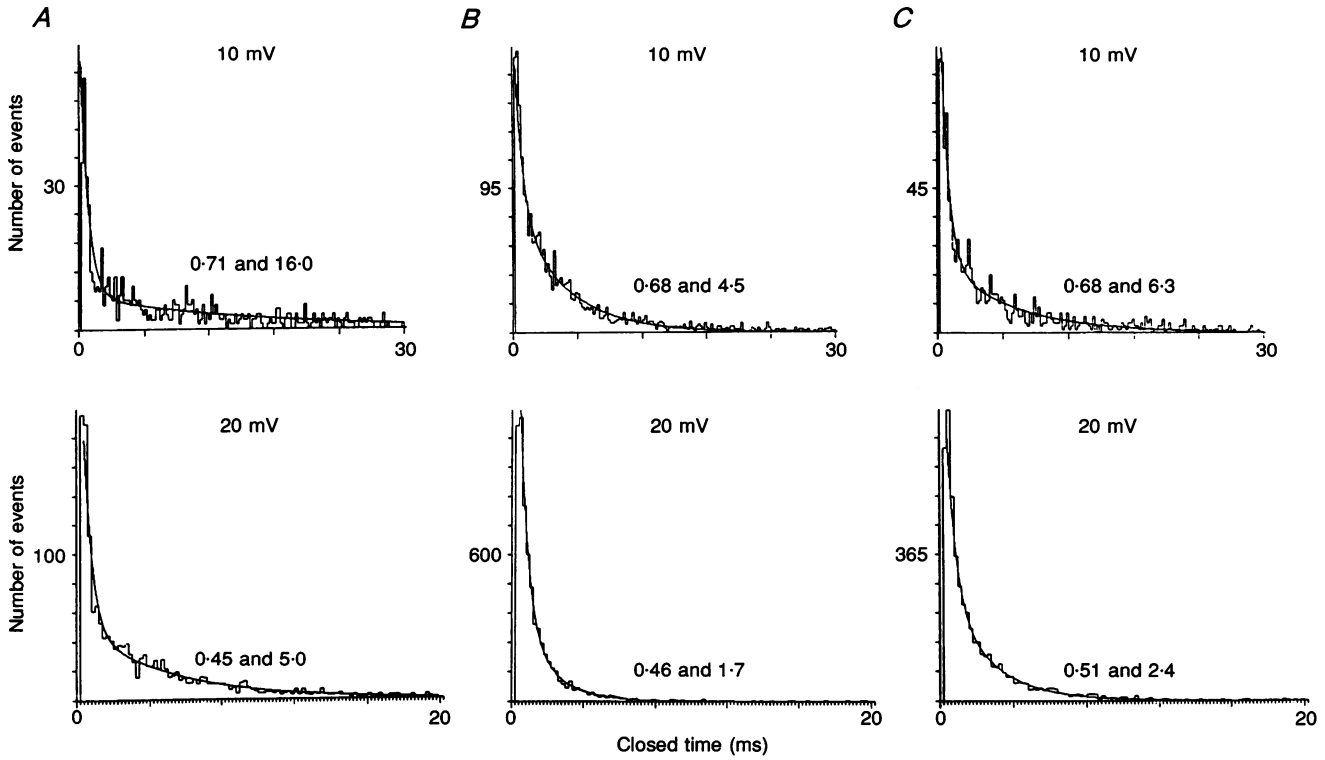

Figure 7. Closed time histograms (from the same patch as shown in Fig. 6)
Panels are specified in the same way as in Fig. 6. Numbers indicate τ_{fast} and τ_{slow} (in ms), obtained by double exponential fittings up to 30 ms at +10 mV and to 20 ms at +20 mV. Numbers of events in the data obtained at 0 mV were not enough for reliable fittings.

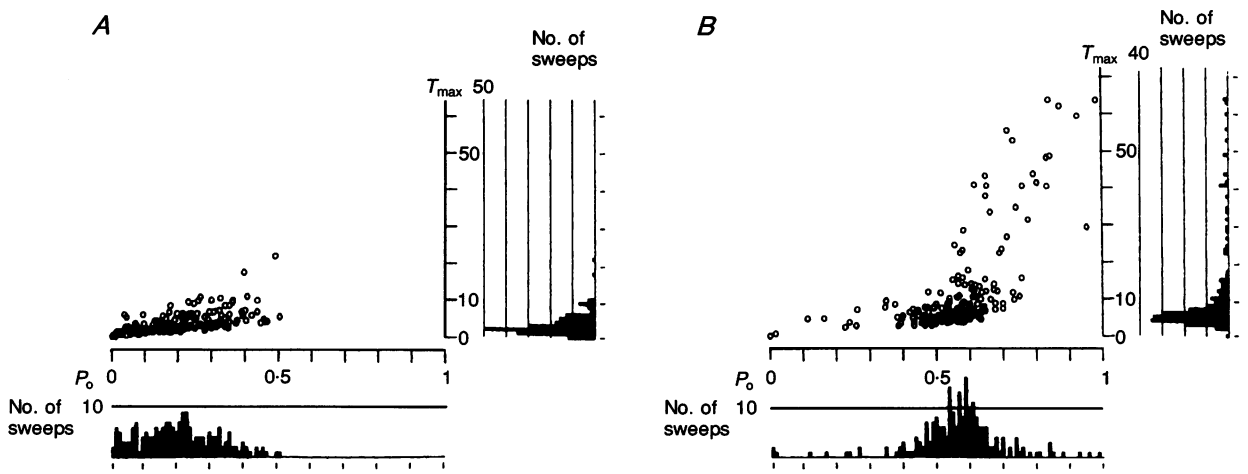

Figure 8. Increase in 'mode 2' gating behaviour during Ca^{2+}-dependent potentiation
This patch was characterized by the high channel activity in the control state. With the elevation of $R_{340/380}$ from 0·28 to 0·51, P_o was increased from 0·16 to 0·48. Distributions of sweeps with channel activity are shown in the $P_o - T_{max}$ plane (*A*, control; *B*, during Ca^{2+}-dependent potentiation). Projections onto the P_o axis (below) showed continuous distribution patterns. Histogram projections onto T_{max} axis are shown to the right of the $P_o - T_{max}$ plane.

remained active in spite of transient Ca^{2+}-dependent inactivation.

Ca^{2+}-dependent suppression of channel activity or 'inactivation' was a consistent finding in six patches where $R_{340/380}$ exceeded unity. In all cases, however, we could observe sporadic channel openings during Ca^{2+}-dependent inactivation.

DISCUSSION

Using Ba^{2+} as the charge carrier, the present study demonstrated at the single-channel current level that tonic changes in $[Ca^{2+}]_i$ modulate cardiac L-type Ca^{2+} channel activity in two opposite ways. When $[Ca^{2+}]_i$ level was altered through changes in $[Ca^{2+}]_o$ under K^+ depolarization, the activity of single L-type Ca^{2+} channels was potentiated with moderate increase in $[Ca^{2+}]_i$ ($R_{340/380}$ around 0·5–0·8 or $[Ca^{2+}]_i$ around 180–400 nM, as estimated from the calibration curve shown in Fig. 1). The channel activity was suppressed with further increase in $[Ca^{2+}]_i$ ($R_{340/380} > 1·0$ or estimated $[Ca^{2+}]_i > 600$ nM). Recognizing problems in the assessment of absolute values for $[Ca^{2+}]_i$ (Wier, 1990; Frampton *et al.* 1991) and those related to heterogeneous distribution of cytosolic Ca^{2+} concentrations (Wier, Cannell, Berlin, Marban & Lederer, 1987; Imredy & Yue, 1992), these $[Ca^{2+}]_i$ levels were apparently in the range of physiological changes during the cardiac cycle.

Contribution by intracellular environments?

L-type Ca^{2+} channels are modulated by complicated regulatory mechanisms, including those mediated by intracellular factors (Reuter, 1983; Eckert & Chad, 1984; Tsien *et al.* 1986; Belles, Malecot, Hescheler & Trautwein, 1988; Trautwein & Hescheler, 1990). It should be stressed, therefore, that currents in this study were recorded in the cell-attached configuration, where the intracellular environment is least disturbed. This may explain discrepancies with previous observations (Rosenberg, Hess & Tsien, 1988; Huang, Quayle, Worley, Standen & Nelson, 1989), where tonic elevations in $[Ca^{2+}]_i$ failed to reveal Ca^{2+}-dependent inactivation at the single-channel level. Recently, however, using excised inside-out patches in the presence of calpastatin, ATP and Bay K 8644, Romanin *et al.* (1992) demonstrated that elevation of Ca^{2+} to micromolar concentrations suppressed Ca^{2+} channel activity. Ca^{2+}-dependent potentiation, on the other hand, has not yet been reported at the single-channel level.

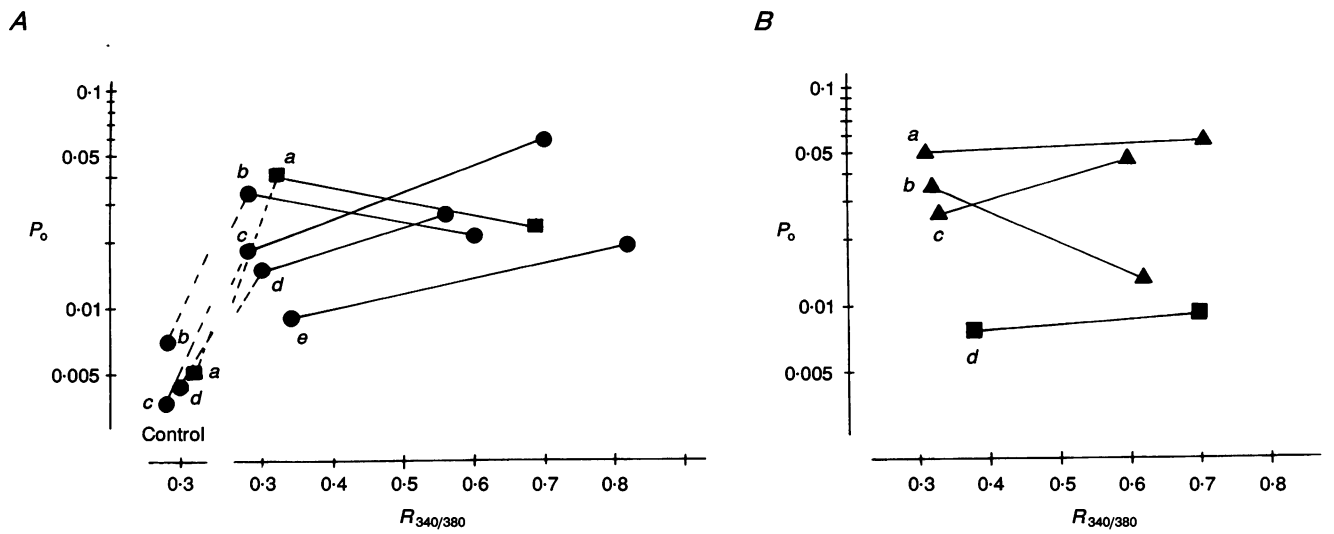

Figure 9. Effects of increased $[Ca^{2+}]_i$ during protein kinase A activation and inhibition
A, relationships between $[Ca^{2+}]_i$ and channel open probability after cAMP-dependent potentiation. Ordinate, P_o on a logarithmic scale after the correction for the number of channels in the patch. Abscissa, $R_{340/380}$. As in Fig. 3, data from the same patch were connected. P_o values before the application of drugs (forskolin for *a*, *c*, *e*; 8-bromocyclic-AMP for *b*; isoprenaline for *d*) are shown on the left, except for *e*, where control activity was not measured. *b* was obtained from a single-channel patch. Changes in kinetic parameters from this patch were as follows for control, increased cAMP and increased $[Ca^{2+}]_i$, respectively: availability, 46·0, 70·4, 48·8%; averaged P_o for non-blank sweeps, 0·015, 0·048, 0·042; τ_{open}, 0·34, 0·58, 0·59 ms; $\tau_{closed,fast}$, 0·91, 1·11, 1·05 ms; and $\tau_{closed,slow}$, 16·7, 11·4, 10·2 ms. *B*, relationships between $[Ca^{2+}]_i$ and channel open probability after inhibition of PKA by H-89. *a* was obtained from a single-channel patch. In this case, increased $[Ca^{2+}]_i$ changed the kinetic parameters as follows: availability, 51·6–63·6%; averaged P_o for non-blank sweeps, 0·098–0·090; τ_{open} 0·75–0·73 ms; $\tau_{closed,fast}$, 0·50–0·48 ms; and $\tau_{closed,slow}$, 4·78–4·55 ms. Symbols indicate different test voltages (●, 0 mV; ■, + 10 mV; ▲, + 20 mV).

Kinetic analysis of unitary current during Ca^{2+}-dependent potentiation

Our single-channel study demonstrated that the Ca^{2+}-dependent potentiation observed previously at the whole-cell current level (Gurney *et al.* 1989) is due to increased probability for channel opening. This is associated with (1) increased number of sweeps with channel openings (channel availability) and (2) increased P_o during non-blank sweeps. In eight cases, summarized in Table 1, the averaged ratio of availability (value during potentiation : control) was $1{\cdot}45 \pm 0{\cdot}38$, while the ratio of P_o for non-blank sweeps amounted to $2{\cdot}83 \pm 1{\cdot}76$.

Our results indicate that both effects were caused by multiple kinetic mechanisms. When the numbers of consecutive non-blank sweeps (T_s) and blank sweeps (T_f) were analysed, increase in T_s and decrease in T_f both contributed to increased availability in five out of eight cases. Increased P_o for non-blank sweeps was produced not only by the graded changes in open and closed time constants, but also by increased numbers of sweeps with unusually long openings or 'mode 2' behaviour at high test voltages. Because there are many Ca^{2+}-dependent processes in intact cells that might affect L-type Ca^{2+} channels (Trautwein & Hescheler, 1990), it is reasonable, or to be expected, that the increase in overall P_o involves several different mechanisms.

We can point out, however, that changes in kinetic behaviour during Ca^{2+}-dependent potentiation share several properties with those observed during β-adrenergic stimulation. Changes in 'slow gating behaviour' or decrease in non-available sweeps are reported during β-stimulation by Ochi & Kawashima (1990). In their report, both an increase in T_s and a decrease in T_f (which is more slight) contributed to increased channel availability. This is similar to our results for Ca^{2+}-dependent potentiation. When open and closed time histograms were analysed, the most striking or consistent effect was the decrease in the slow component of closed time constants ($\tau_{closed,slow}$). This is also the case when the effects of cyclic-AMP (Cachelin, de Peyer, Kokubun & Reuter, 1983) or a β-agonist (Brum, Osterrieder & Trautwein, 1984) were examined. Furthermore, Yue *et al.* (1990) have recently confirmed that the high-activity gating mode is potentiated during β-adrenergic stimulation. The distribution of P_o after 'mode 2' potentiation (Fig. 8*B*) was more like their case (see Fig. 2 in Yue *et al.* 1990) than that after the application of dihydropyridine calcium agonist (Hess *et al.* 1984). A similar effect was seen by Ono & Fozzard (1993) with high doses of okadaic acid, a blocker of the phosphatase reaction.

In cardiac myocytes, mechanisms linked to channel phosphorylation by cAMP-dependent protein kinase have been suggested for Ca^{2+}-dependent stimulatory effects by Gurney *et al.* (1989) and Charnet, Richard, Gurney, Ouaid, Tiaho & Nargeot (1991), although this view was not supported in their recent reports on guinea-pig ventricular myocytes (Bates & Gurney, 1993; see later). On the other hand, Ca^{2+}-dependent enhancement in smooth muscle cells is reported to be caused by calmodulin-dependent

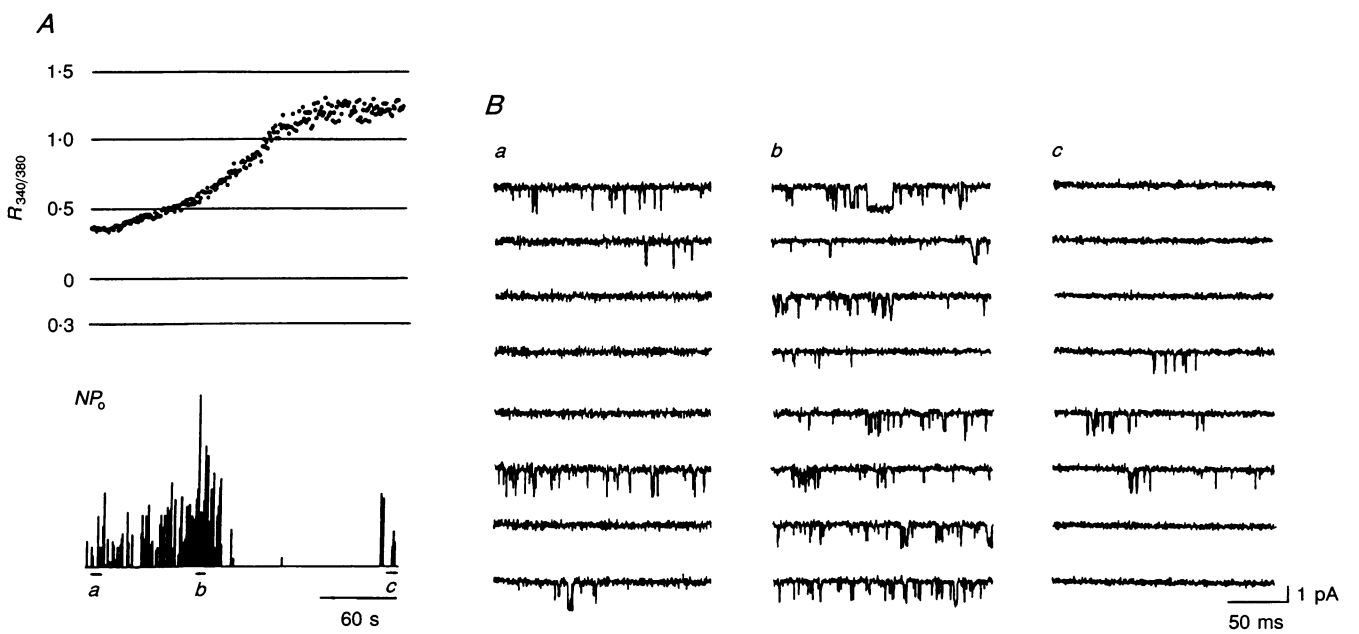

Figure 10. $[Ca^{2+}]_i$-dependent inactivation of Ca^{2+} channels
A, temporal profiles of $R_{340/380}$ and NP_o. Depolarizing pulses were delivered to 0 mV at 1 Hz. Increase in extracellular Ca^{2+} caused the elevation of $R_{340/380}$ above unity. *B*, original current traces during the period indicated by bars in *A*.

protein kinase II (McCarron, McGeown, Reardon, Ikebe, Fay & Walsh, 1992). Our attempts to clarify the relationships between PKA-dependent modulation of Ca^{2+} channels and the $[Ca^{2+}]_i$ effect were not fully conclusive because the behaviour of the channels was variable from one patch to another (Fig. 9). As shown in Fig. 3, channel activities in individual patches already showed considerable variations in the control state in our experimental condition. This is presumably due to the diversity of intracellular metabolic factors of myocytes, including those to control the phosphorylation of channel protein. Consequently, interventions to stimulate or inhibit PKA activity are highly likely to exaggerate cell-to-cell diversities. We could demonstrate, however, that several channels failed to show Ca^{2+}-dependent potentiation after cAMP-dependent phosphorylation (Fig. 9*A*) or after suppression of PKA by H-89 (Fig. 9*B*). These results are in contrast to the experiments without interventions, where Ca^{2+}-dependent potentiation was an invariable finding (Fig. 3). During the series of experiments to examine the PKA effects, we obtained two recordings with only one channel in the patch (*b* in Fig. 9*A* and *a* in Fig. 9*B*). In spite of changes in $[Ca^{2+}]_i$, kinetic analysis of these data yielded minimal changes in gating

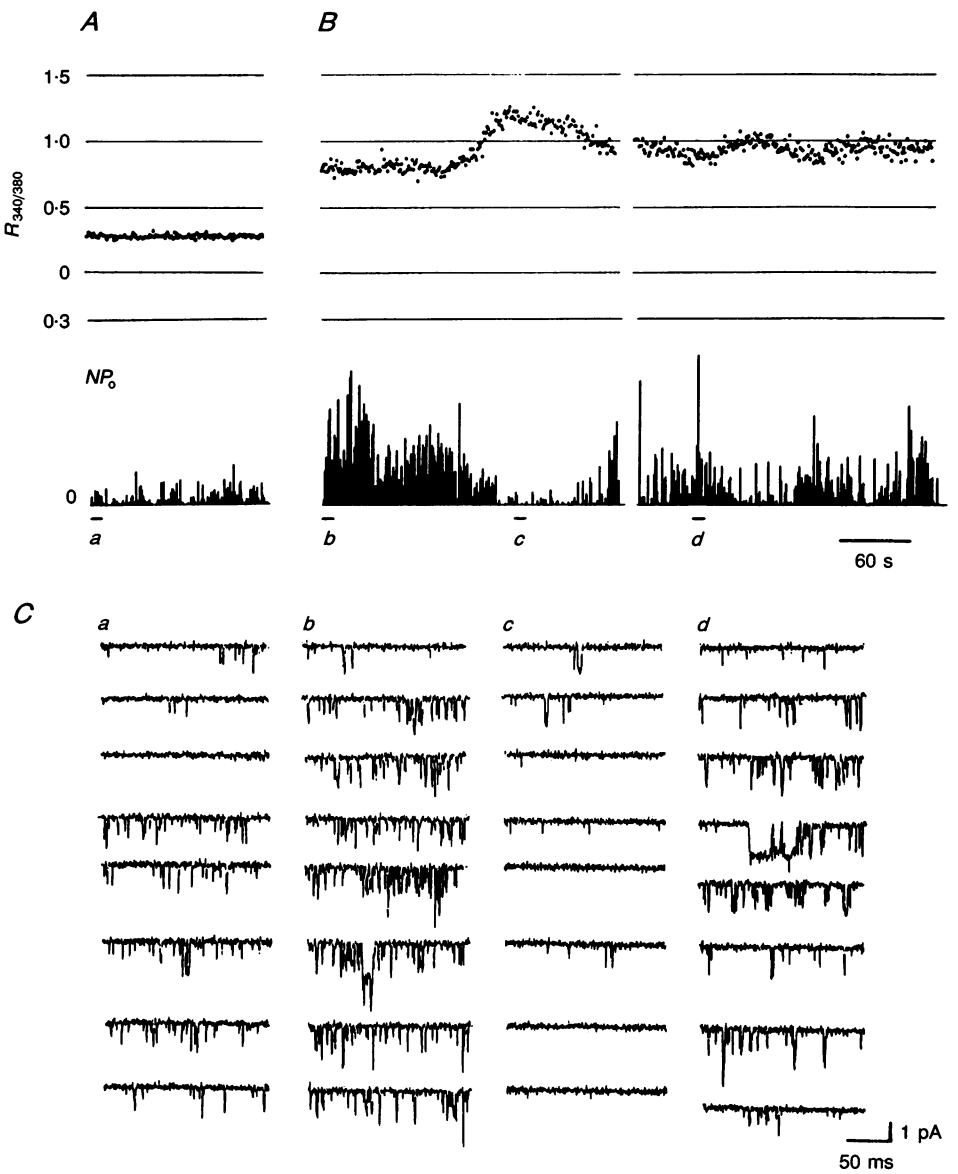

Figure 11. High $[Ca^{2+}]_i$ induced transient reduction in channel activity
A, control; *B*, about 10 min after the bath solution was switched to Ca^{2+}-containing solution. Top panels show $R_{340/380}$ and bottom panels show NP_o during each depolarizing pulse to 0 mV delivered at 1 Hz. *C*, unitary current records during the period indicated by bars in *A* and *B*.

time constants, including $\tau_{closed,slow}$ (see legend to Fig. 9). This again showed a sharp contrast to the cases without interventions, where a decrease in $\tau_{closed,slow}$ was a consistent finding (Table 1).

Thus, our results support the view that PKA-dependent phosphorylation of the channel protein contributes to increased channel activity during Ca^{2+}-dependent potentiation, although it may not be the sole factor. Recently, Bates & Gurney (1993) suggested that in guinea-pig ventricular myocytes, the potentiation was not mediated by Ca^{2+}-dependent phosphorylation, but it did involve a nucleotide (O'Rourke, Backx & Marban, 1992). This conclusion was based on the observation that intracellularly applied protein kinase inhibitors H-7 and Rp-cAMP-S had no significant effect on the photolysis-induced potentiation. We feel that this discrepancy can partly be explained by the difference in intracellular environment. During whole-cell recording, the inside of the cell membrane is exposed to an artificially controlled pipette solution. On the other hand, it is expected to be least disturbed during cell-attached recordings, as used in our case. Further studies are necessary to confirm (or rule out) the involvement of channel phosphorylation cycles during Ca^{2+}-dependent modulation of Ca^{2+} channel in mammalian cardiac myocytes.

Physiological implications

$[Ca^{2+}]_i$ levels required for Ca^{2+}-dependent potentiation and inactivation were found in the range that cardiac myocytes span during physiological cardiac cycles. Our results further indicate that these two opposite effects have different temporal profiles, which appear to be relevant for their physiological functions. Quick responses in Ca^{2+}-dependent inactivation might be necessary to protect myocytes from excess intracellular Ca^{2+} loading. When Ca^{2+} is the charge carrier, as in physiological conditions, Ca^{2+}-dependent inactivation of Ca^{2+} channels is further affected by Ca^{2+} entering through the channel pore (Imredy & Yue, 1992; see also Mazzanti, DeFelice & Liu, 1991). On the other hand, Ca^{2+}-dependent potentiation contributes to modulation of channel activity on a more prolonged time scale. Consistent with the report in smooth muscle cells (McCarron *et al.* 1992), Ca^{2+}-dependent potentiation in heart cells had a sustained nature (Fig. 2). Furthermore, this potentiation was resistant to transient Ca^{2+}-induced inactivation, as shown in Fig. 11. A persistent effect in Ca^{2+}-dependent potentiation following a moderate increase in the $[Ca^{2+}]_i$ level gives support to interpretations of previous studies, including those on the effects of repetitive stimulations (Fedida *et al.* 1988; Zygmunt & Maylie, 1990) and on the channel recovery process (Tseng, 1989). In these non-steady states, Ca^{2+}-dependent modulations of L-type Ca^{2+} channels may also contribute to a variety of changes in the inotropic state of cardiac muscle.

REFERENCES

Bates, S. E. & Gurney, A. M. (1993). Ca^{2+}-dependent block and potentiation of L-type calcium current in guinea-pig ventricular myocytes. *Journal of Physiology* **466**, 345–363.

Belles, B., Malecot, C. O., Hescheler, J. & Trautwein, W. (1988). 'Run-down' of the Ca current during long whole-cell recordings in guinea-pig heart cells: role of phosphorylation and intracellular calcium. *Pflügers Archiv* **411**, 353–360.

Brum, G., Osterrieder, W. & Trautwein, W. (1984). β-Adrenergic increase in the calcium conductance of cardiac myocytes studied with the patch clamp. *Pflügers Archiv* **401**, 111–118.

Cachelin, A. B., De Peyer, J. E., Kokubun, S. & Reuter, H. (1983). Ca^{2+} channel modulation by 8-bromocyclic AMP in cultured heart cells. *Nature* **304**, 462–464.

Cavalier, A., Pelzer, D. & Trautwein, W. (1986). Fast and slow gating behaviour of single calcium channels in cardiac cells. *Pflügers Archiv* **406**, 241–258.

Charnet, P., Richard, S., Gurney, A. M., Ouaid, H., Tiaho, F. & Nargeot, J. (1991). Modulation of Ca currents in isolated frog atrial cells studied with photosensitive probes. Regulation by cAMP and Ca^{2+}: A common pathway? *Journal of Molecular and Cellular Cardiology* **23**, 343–356.

Eckert, R. & Chad, J. E. (1984). Inactivation of Ca channels. *Progress in Biophysics and Molecular Biology* **44**, 215–267.

Fedida, D., Noble, D. & Spindler, A. J. (1988). Mechanism of the use dependence of Ca^{2+} current in guinea-pig myocytes. *Journal of Physiology* **405**, 461–475

Fenwick, E. M., Marty, A. & Neher, E. (1982). Sodium and calcium channels in bovine chromaffin cells. *Journal of Physiology* **331**, 599–635.

Frampton, J. E., Orchard, C. H. & Boyett, M. R. (1991). Diastolic, systolic and sarcoplasmic reticulum $[Ca^{2+}]$ during inotropic interventions in isolated rat myocytes. *Journal of Physiology* **437**, 351–375.

Grynkievicz, G., Poenie, M. & Tsien, R. Y. (1985). A new generation of Ca^{2+} indicators with greatly improved fluorescence properties. *Journal of Biological Chemistry* **260**, 3440–3450.

Gurney, A. M., Charnet, P., Pye, J. M. & Nargeot, J. (1989). Augmentation of cardiac calcium current by flash photolysis of intracellular caged-Ca^{2+} molecules. *Nature* **341**, 65–68.

Hadley, R. W. & Lederer, W. J. (1991). Ca^{2+} and voltage inactivate Ca^{2+} channels in guinea-pig ventricular myocytes through independent mechanisms. *Journal of Physiology* **444**, 257–268.

Hamill, O. A., Marty, A., Neher, E., Sakmann, B. & Sigworth, F. J. (1981). Improved patch-clamp techniques for high-resolution current recording from cells and cell-free membrane patches. *Pflügers Archiv* **391**, 85–100.

Hess, P., Lansman, J. B. & Tsien, R. W. (1984). Different modes of Ca channel gating behaviour favoured by dihydropyridine Ca agonists and antagonists. *Nature* **311**, 538–544.

Hirano, Y., Abe, S., Sawanobori, T. & Hiraoka, M. (1991). External ATP-induced changes in $[Ca^{2+}]_i$ and membrane currents in mammalian atrial myocytes. *American Journal of Physiology* **260**, C673–680.

Hirano, Y., Fozzard, H. A. & January, C. T. (1989). Characteristics of L- and T-type Ca currents in canine cardiac Purkinje cells. *American Journal of Physiology* **256**, H1478–1492.

Hirano, Y. & Hiraoka, M. (1988). Barium-induced automatic activity in isolated ventricular myocytes from guinea-pig hearts. *Journal of Physiology* **395**, 455–472.

Huang, Y., Quayle, J. M., Worley, J. F., Standen, N. B. & Nelson, M. T. (1989). External cadmium and internal calcium block of single calcium channels in smooth muscle cells from rabbit mesenteric artery. *Biophysical Journal* **56**, 1023–1028.

IMREDY, J. P. & YUE, D. T. (1992). Submicroscopic Ca^{2+} diffusion mediates inhibitory coupling between individual Ca channels. *Neuron* **9**, 197–207.

ISENBERG, G. & KLOCKNER, V. (1982). Calcium tolerant ventricular myocytes prepared by preincubation in a 'KB medium'. *Pflügers Archiv* **395**, 6–18.

KASS, R. S. & SANGUINETTI, M. C. (1984). Inactivation of calcium channel current in the calf cardiac Purkinje fibre: Evidence for voltage- and calcium-mediated mechanism. *Journal of General Physiology* **84**, 705–726.

LEE, K. S., MARBAN, E. & TSIEN, R. W. (1985). Inactivation of calcium channels: Joint dependence on membrane potential and intracellular calcium. *Journal of Physiology* **364**, 395–411.

LI, Q., ALTSCHULD, R. A. & STOKES, B. T. (1987). Quantitation of intracellular free calcium in single adult cardiomyocytes by fura-2 fluorescence microscopy: calibration of fura-2 ratios. *Biochemical and Biophysical Research Communications* **147**, 120–126.

MCCARRON, J. G., MCGEOWN, J. G., REARDON, S., IKEBE, M., FAY, F. S. & WALSH, J. V. (1992). Calcium-dependent enhancement of calcium current in smooth muscle by calmoduline-dependent protein kinase II. *Nature* **357**, 74–77.

MARBAN, E. & TSIEN, R. W. (1982). Enhancement of calcium current during digitalis inotropy in mammalian heart: positive feed-back regulation by intracellular calcium? *Journal of Physiology* **329**, 589–614.

MAZZANTI, M., DEFELICE, L. J. & LIU, Y. (1991). Gating of L-type Ca^{2+} channels in embryonic chick ventricle cells: dependence on voltage, current and channel density. *Journal of Physiology* **443**, 307–334.

OCHI, R. & KAWASHIMA, Y. (1990). Modulation of slow gating process of calcium channels by isoprenaline in guinea-pig ventricular cells. *Journal of Physiology* **424**, 187–204.

ONO, K. & FOZZARD, H. A. (1993). Two phosphatase sites on the Ca channel affecting different kinetic functions. *Journal of Physiology* **470**, 73–84.

O'ROURKE, B., BACKX, P. H. & MARBAN, E. (1992). Phosphorylation-independent modulation of L-type calcium channels by magnesium–nucleotide complexes. *Science* **257**, 245–248.

PIETROBON, D. & HESS, P. (1990). Novel mechanism of voltage-dependent gating in L-type calcium channels. *Nature* **346**, 651–655.

REUTER, H. (1983). Calcium channel modulation by neurotransmitters, enzymes and drugs. *Nature* **301**, 569–574.

ROMANIN, C., KARLSSON, J. O. & SCHINDLER, H. (1992). Activity of cardiac L-type Ca channels is sensitive to cytoplasmic calcium. *Pflügers Archiv* **421**, 516–518.

ROSENBERG, R. L., HESS, P. & TSIEN, R. W. (1988). Cardiac calcium channels in planar lipid bilayers. L-type channels and calcium permeable channels open at negative membrane potentials. *Journal of General Physiology* **92**, 27–54.

TRAUTWEIN, W. & HESCHELER, J. (1990). Regulation of cardiac L-type calcium current by phosphorylation and G proteins. *Annual Review of Physiology* **52**, 257–274.

TSENG, G.-N. (1989). Calcium current restitution in mammalian ventricular myocytes is modulated by intracellular calcium. *Circulation Research* **63**, 468–482.

TSIEN, R. W., BEAN, B. P., HESS, P., LANSMAN, J. B., NILIUS, B. & NOWYCKY, M. C. (1986). Mechanism of calcium channel modulation by β-adrenergic agents and dihydropyridine calcium agonists. *Journal of Molecular and Cellular Cardiology* **18**, 691–710.

WIER, W. G. (1990). Cytoplasmic $[Ca^{2+}]$ in mammalian ventricle: Dynamic control by cellular processes. *Annual Review of Physiology* **52**, 467–485.

WIER, W. G., CANNELL, M. B., BERLIN, J. R., MARBAN, E. & LEDERER, W. J. (1987). Cellular and subcellular heterogeneity of $[Ca^{2+}]_i$ in single heart cells revealed by fura2. *Science* **235**, 325–328.

WILLIAMS, D. A., FOGARTY, K. E., TSIEN, R. Y. & FAY, F. S. (1985). Calcium gradients in single smooth muscle cells revealed by the digital imaging microscope using Fura-2. *Nature* **318**, 358–361.

YUE, D. T., HERZIG, S. & MARBAN, E. (1990). β-Adrenergic stimulation of calcium channels occur by potentiation of high-activity gating modes. *Proceedings of the National Academy of Science of the USA* **87**, 753–757.

ZYGMUNT, A. C. & MAYLIE, J. (1990). Stimulation-dependent facilitation of the high threshold calcium current in guinea-pig ventricular myocytes. *Journal of Physiology* **428**, 653–671.

Acknowledgements

The authors thank Dr H. A. Fozzard for his critical reading of the manuscript. This work was supported by a grant (No. 03670443) from the Ministry of Education, Science and Culture of Japan.

Received 4 March 1993; accepted 18 March 1994.